Scale-Dependent Rotational Diffusion Of Nanoparticles In Polyethylene Glycol Solutions

Lorena Maldonado-Camargo[1], Chuncheng Yang[2] and Carlos Rinaldi[1,2*]

[1]Department of Chemical Engineering, University of Florida, P.O. Box 116005, Gainesville, FL 32603

[2]J. Crayton Pruitt Family Department of Biomedical Engineering, P.O. Box 116131, Gainesville, FL 32611

*Author to whom correspondence should be addressed, J. Crayton Pruitt Family Department of Biomedical Engineering, P.O. Box 116131, Gainesville, FL 32611 Fax: (352) 273-9221. Tel.: (352) 294-5588. E-mail: carlos.rinaldi@bme.ufl.edu

Polymer characterization. The steady state viscosity of the PEG melts was measured at 298 K using an Anton Paar MCR 302 rheometer with cup and bob geometry. During each measurement, the sample was pre-shear at 1 1/s during 5 min, followed by a shear rate ramp from 10 to 1000 s-1 to measure the viscosity. Figure SI-1 shows the viscosity of each polymer as a function of shear rate and at different temperatures. The results indicate that the solution prepared with PEG 2 kDa to PEG 17 kDa behave as Newtonian fluids in the experimental shear rate range. At high concentration, samples prepared with PEG 197 kDa and PEG 363 kDa exhibit a shear thinning behavior at high shear rates. It is important to remark that, even though the solutions prepared with high molecular PEGs (higher than 100 kDa and above the overlap concentration) exhibited a shear-thinning behavior, the MNPs in the polymer solutions behave as in a Newtonian fluid since the DMS spectra continue to follow the Debye model (see Figure SI-1e and Figure SI-1f).

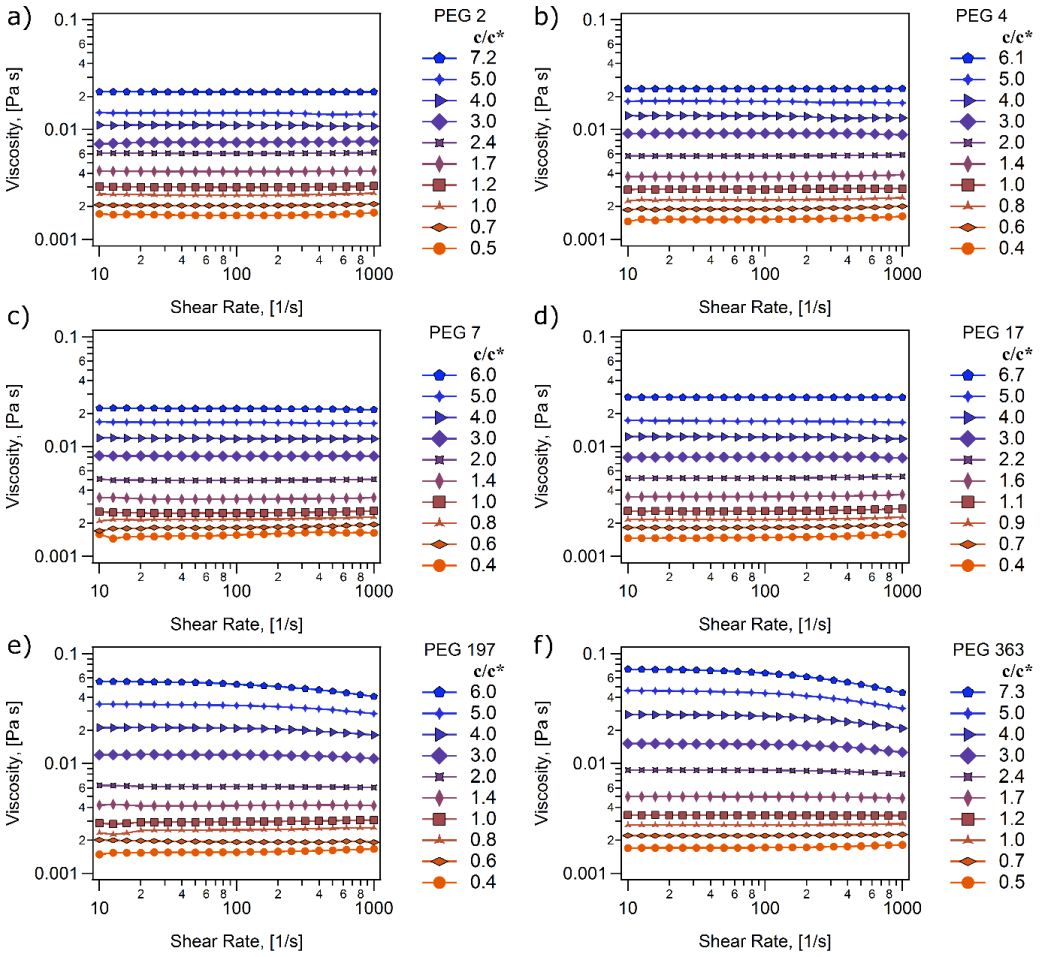

Figure SI-1. Viscosity of PEG solutions as a function of shear rate at 298 K measured in a rheometer.

The overlap concentration for each polymer was also estimated from measurements of the intrinsic viscosity of the solutions, extrapolated to infinite dilution. Figure SI-2 shows these measurements, along with fits used to obtain the y-axis intercept, which is the inverse of the overlap concentration. The results are tabulated in Table SI-1, which also includes the theoretical values obtained using the equation $c^* = 3M_n / 4\pi R_g^3 N_A$, as well as the relative error between the experimental and theoretical values. The relative error between the theoretical and experimental value is relatively small and as such this value was used throughout the manuscript.

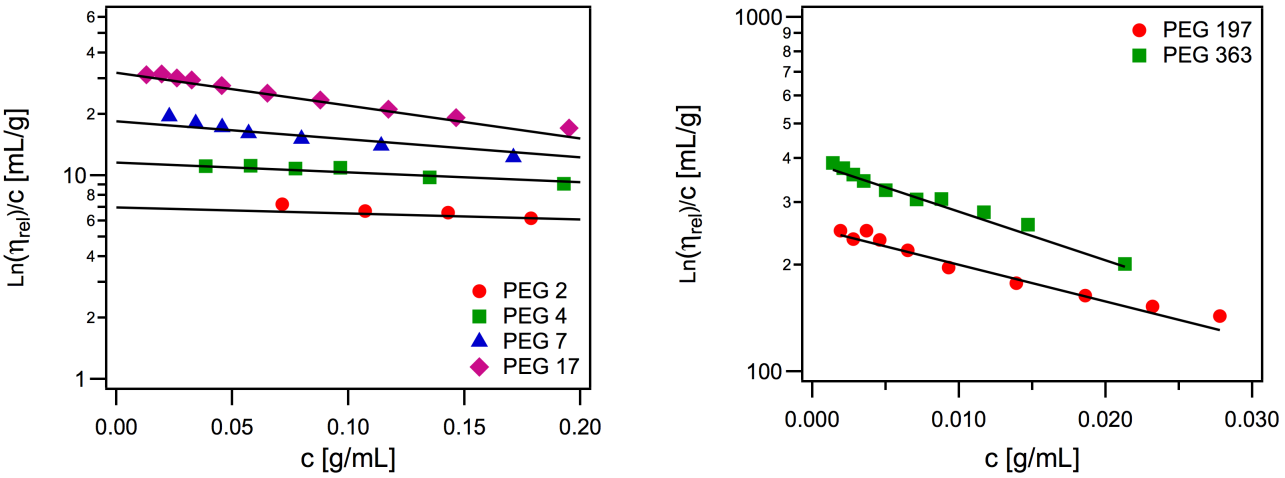

Figure SI-2. $\ln(\eta_{rel})/c$ *vs* c to calculate the intrinsic viscosity of polymer solutions prepared with PEG polymer a) 2, 4, 7 and 17, and b) 197 and 363.

Table SI-1. Intrinsic viscosity and overlap concentration calculations for PEG polymer solutions.

PEG	Intercept [mL/g]	Overlap concentration [g/mL]		% Error
		Measured	Theoretical	
2	6.96181	0.1436	0.1498	4.2%
4	11.5665	0.0865	0.0948	9.2%
7	18.4563	0.0542	0.0570	5.0%
17	31.8898	0.0314	0.0293	6.9%
197	241.751	0.0040	0.0046	14.0%
363	382.817	0.0026	0.0029	10.9%

Determination of overlap regime. Polymer solutions in the semidilute regime can be classified as being in the semidilute unentangled and semidilute entangled regime depending on their concentration.[1] The entanglement volume fraction was estimated using $c_e = \phi_e M_0 / b^3 N_A$, with $\phi_e \approx \left[N_e(1)/N\right]^{3/4}$ (this is the expression for θ-solvents,[1] but the numerical results are very similar for athermal solvent), where $N_e(1)$ is the number of Kuhn monomers in an entanglement strand in the melt, N is the number of Kuhn monomers in the polymer chain, M_0 is the molecular weight of a Kuhn segment (137 g/mol for PEG[1]), b is the statistical length of a Kuhn segment (1.1. nm for PEG[1]), and N_A is Avogadro's constant. Table SI-2 summarizes the calculation results. From the results of Table SI-2 it is seen that the majority of the solutions in the semidilute regime are in the entangled semidilute regime.

Table SI-2. Entanglement concentration calculation results for PEG solutions.

PEG	M_n [kg/mol]	N	c_e [g/mL]	c_e/c^*
2*	1.9	13.9	0.176	1.17
4	3.5	25.5	0.1129	1.19
7	6.9	50.4	0.0672	1.18
17	16.8	122.6	0.0345	1.18
197	196.7	1436	0.0054	1.17
363	363.1	2560	0.00344	1.19

*We note that for PEG 2, the molecular weight of the polymer is close to the entanglement strand molecular weight of 2 kg/mol in the melt.[2]

Dynamic Magnetic Susceptibility (DMS) Measurements. DMS measurements of particles suspended in the polymer solutions were obtained using an Acreo Dynomag AC susceptometer. During the measurements, a constant field of 5 Gauss (397.89 A m^{-1}) is applied and the frequency of the applied field is swept in a range of 10 Hz to 100 kHz. 200 µL of the particle suspensions were used for analysis at room temperature (298 K).

Figure SI-3 shows examples of the DMS spectra of the particles in polymer solutions of different molecular weights. Here we only show the samples with the highest concentration to demonstrate that follow the Debye model. Similar behavior was observed for the samples with lower concentration.

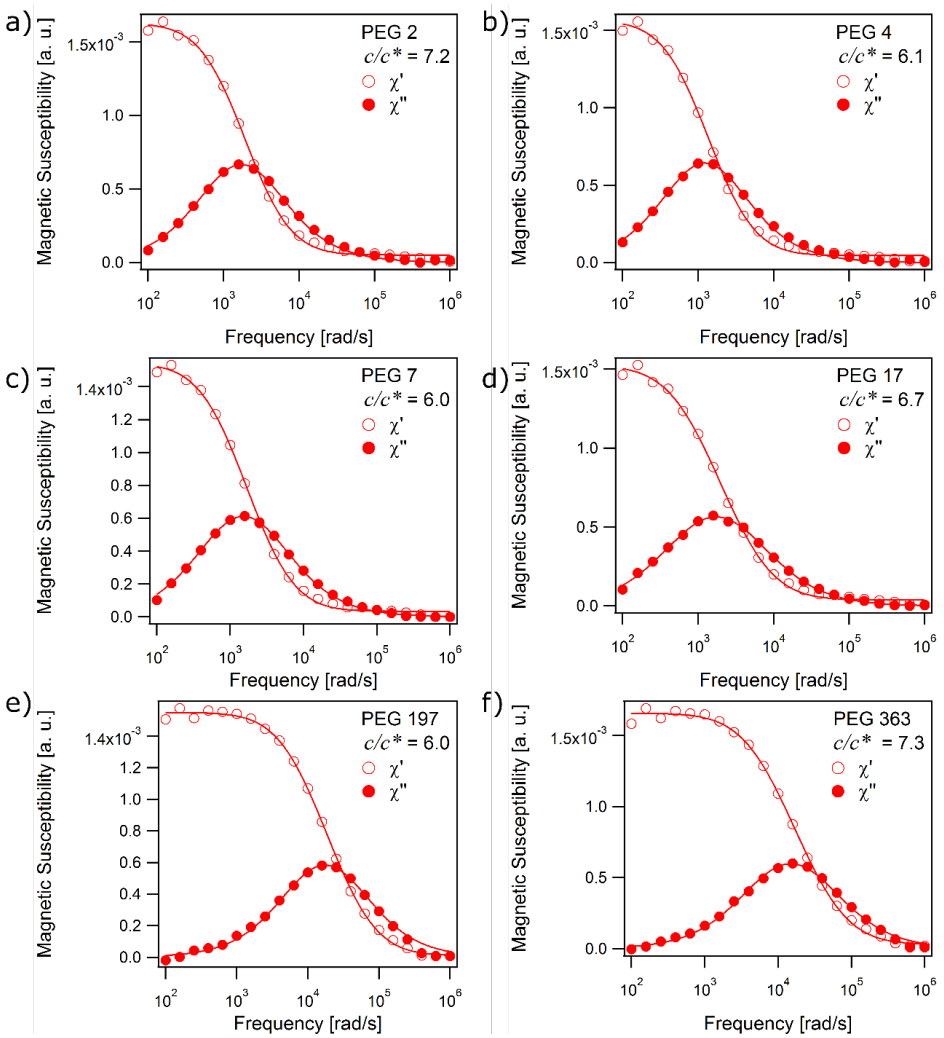

Figure SI-3. DMS measurements of PEG-grafted MNPs in PEG solutions prepared with a) PEG 2, b) PEG 4, c) PEG 7, d) PEG 17, e) PEG 197, and d) PEG 363 at the highest concentration *c/c** room temperature, showing the Debye behavior.

Reproducibility of the observed breakdown of the Stokes-Einstein relation for the rotational diffusivity. Additional measurements were carried out with two more batches of cobalt ferrite nanoparticles coated with PEG of different molecular weights (2 kg/mol and 5 kg/mol), resulting in different hydrodynamic radii. Figure SI-4 shows the hydrodynamic diameters of the two particles. Figure SI-5 compares measured and theoretical rotational diffusivities for the two particles in solutions of four different PEG molecular weights, and Figure SI-6 shows the ratio of experimental to Stokes-Einstein diffusivity for the two particles as a function of concentration in the four PEG solutions. These results are similar to those in the main manuscript for the larger set of polymer molecular weights.

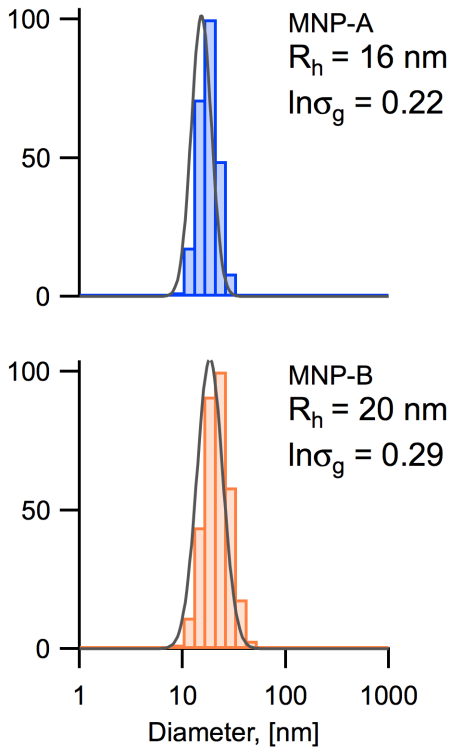

Figure SI-4. Hydrodynamic diameter distributions for two additional PEG-coated cobalt ferrite nanoparticle batches used to test reproducibility of results. MNP-A is coated with PEG 2 kg/mol and MNP-B is coated with PEG 5 kg/mol.

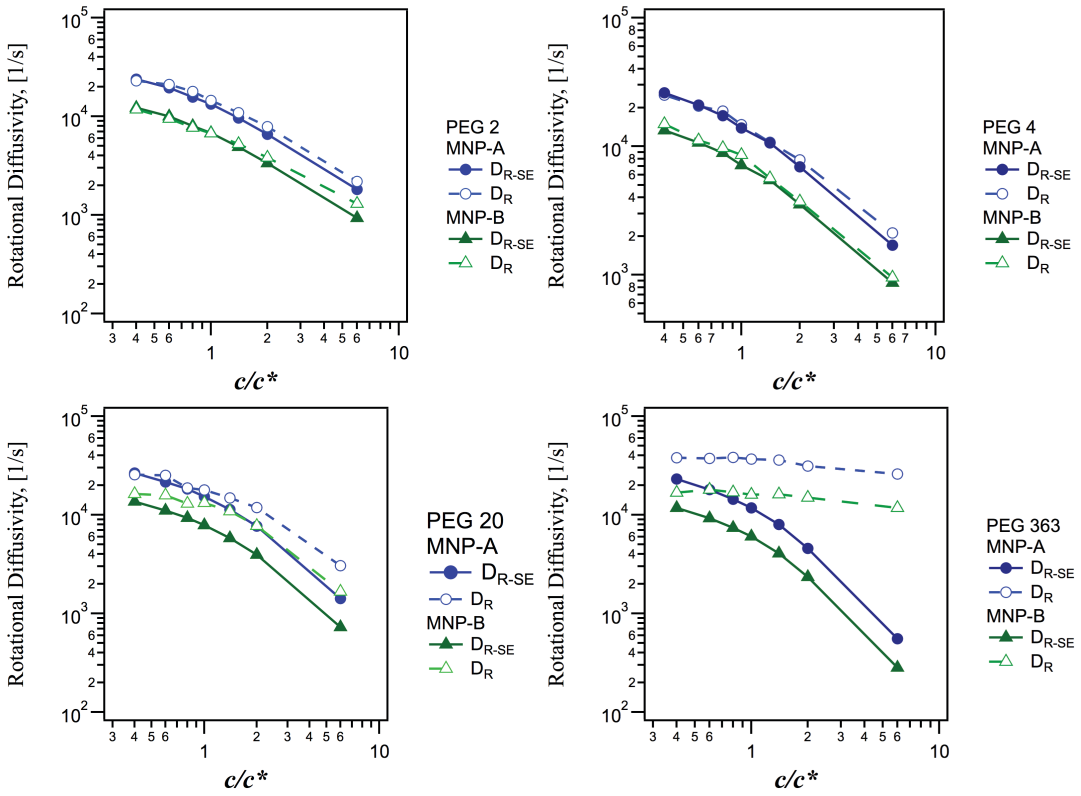

Figure SI-5. Measured (D_R) and predicted ($D_{R\text{-}SE}$) rotational diffusivities for the two PEG-coated nanoparticles of Figure R2 as a function of the concentration of PEG in solution for four different molecular weights. Note that the SE relation accurately predicts the rotational diffusivity for the flow molecular weight polymers (2 and 4.6 kg/mol), begins to show deviations for the intermediate molecular weight (20 kg/mol), and appears to break down for the highest molecular weight (400 kg/mol).

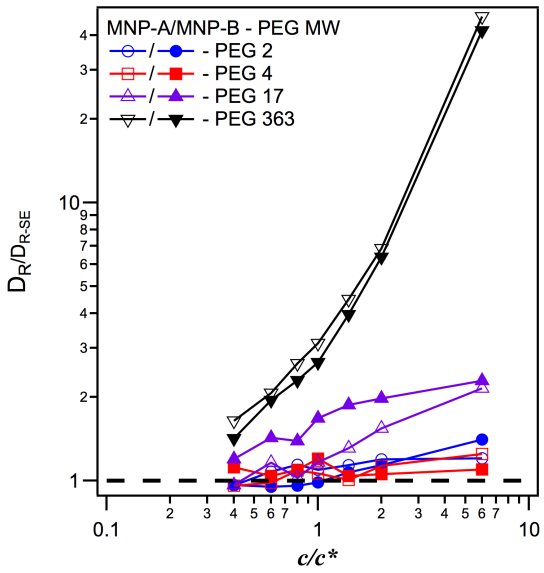

Figure SI-6. Ratio of experimental to predicted rotational diffusivity for the two particles in Figure R3 as a function of concentration of polymer in solution. This graph shows the same behavior as Figure 5 in the manuscript, showing reproducibility of the results.

Potential mechanisms for deviations from predictions of the Stokes-Einstein relation.

Compression of the grafted polymer layer. The observed deviation from predictions by the SE relation may be attributed to the compression of the polymer grafted on the particle surface. Taking into consideration that as c/c^* increased the fraction of the solvent present in solution decreases, one would expect that the polymer grafted on the particle surface tends to shrink. To account for changes in the configuration of the grafted polymer, we calculated the hydrodynamic radius of the nanoparticles assuming that the SE relation in Eq. (1) from the main document accurately predicts the rotational diffusion coefficient based on the viscosity measured in the rheometer. Table SI-3 summarizes the results of these calculations.

Table SI-3. Effective hydrodynamic radius calculated using the Stokes-Einstein relation and the macroscopic (rheometer) viscosity of the solutions.

	PEG 2	PEG 4	PEG 7	PEG 17	PEG 197	PEG 363
c/c^*	r_{p-eff} [nm]	r_{p-eff} [nm]	r_{p-eff} [nm]	r_{p-eff} [nm]	r_{p-eff} [nm]	r_{p-eff} [nm]
0.4	20.6	20.4	18.8	19.4	17.5	17.6
0.6	20.6	20.3	18.3	18.7	16.3	16.4
0.8	20.5	20.3	18.3	18.1	15.2	15.0
1.0	20.2	19.9	19.0	18.1	14.5	14.2
1.4	20.2	20.1	19.1	17.6	12.6	12.4
2.0	19.9	20.2	19.8	17.2	12.0	10.9
3.0	19.4	20.3	19.9	16.4	10.2	9.3
4.0	19.7	20.3	20.7	16.6	8.8	8.0
5.0	20.2	20.4	21.0	17.3	7.8†	7.0†
6.0	20.5	20.9	20.4	18.0	7.0†	6.4†

†Hydrodynamic diameter smaller than the core radius of the nanoparticles determined by TEM.

In solutions prepared with PEG 197 and PEG 363, where the SE relation fails to predict the rotational diffusion of the nanoparticles, as the polymer concentration increases the hydrodynamic radius of the nanoparticles would have to significantly decrease, suggesting possible compression of the grafted polymer. However, we note that at the highest concentrations, when $c/c^* > 5.0$, the nanoparticle's effective hydrodynamic radius would have to be smaller than the radius of the inorganic cores, as measured by TEM. Thus, even though it is possible that the configuration of the grafted polymer may change due to increasing polymer volume fraction, we believe this phenomenon is unable to wholly explain the observed deviation of the experimental rotation diffusion coefficient of the nanoparticles from the predictions of the SE relation.

Effect of polymer correlation length. The correlations length, defined as the average distance from a monomer on one chain to the nearest monomer on another chain[1] and estimated by using the relationship $\xi = R_g \left(c/c^*\right)^{-0.75}$ is a function of the polymer concertation and the radius of gyration of the polymer.

Table SI-4. Calculated correlation lengths for PEG solutions.

c/c^* [approx.]	PEG 2 ξ [nm]	PEG 4 ξ [nm]	PEG 7 ξ [nm]	PEG 17 ξ [nm]	PEG 197 ξ [nm]	PEG 363 ξ [nm]
0.4	3.0	4.8	7.2	11.2	50.9†	63.14†
0.6	2.2	3.5	5.3	8.3	37.6†	46.58†
0.8	1.8	2.9	4.3	6.7	30.3†	37.54†
1.0	1.5	2.4	3.6	5.6	25.6†	31.76†
1.4	1.2	1.9	2.8	4.4	19.9	24.67
2.0	0.9	1.4	2.2	3.4	15.2††	18.88
3.0	0.8	1.1	1.6	2.7	11.2††	16.06††
4.0	0.6	0.9	1.3	2.2	9.1††	12.95††
5.0	0.5	0.7	1.1	1.8	7.7††	10.95††
6.0	0.4	0.6	0.9	1.5	6.7††3	8.28††

†Correlation length ξ values larger than the particle hydrodynamic radius

††Correlation length ξ values smaller than the particle hydrodynamic radius

Comparison to other hydrodynamic models. In semi-dilute solutions of unentangled polymer, the empirical relation between the polymer concentration and the probe hydrodynamic diameter $\eta = \eta_0 \exp\left(K r_p^{\mu} c^{\nu}\right)$ has been widely used to predict the viscosity experienced by the nanoparticle.[4] Here, η_0 is the solvent viscosity, c is the polymer concentration and K, μ and, ν are constants whose values vary from system to system. Following these ideas, recent models suggest that the nanoparticle diffusivity scales as $D_0/D = \exp\left(a\left(L/\xi\right)^b\right)$ where D_0 is the rotational diffusion coefficient of the nanoparticles in pure solvent, a and b are experimental parameters, and L is a function of the particle radius r_p and/or R_g.[3, 5, 6]

In Figure SI-4 we compare the experimentally measured relative diffusivities $\ln\left(D_{R-0}/D_R\right)$ to the hydrodynamic model proposed by Holyst *et al.*[7] assuming R_g/ξ as the characteristic length. We see that the diffusivities do not collapse onto a single curve as a function of R_g/ξ (Figure SI-4). Only the diffusivities for polymers with a radius of gyration smaller than the radius of gyration of the nanoparticles $\left(r_p/R_g > 1\right)$ collapse onto a single curve as a function of R_g/ξ (Figure SI-4). The experimental parameters $a = 1.04$ and $b = 0.77$ are similar to those reported by Holyst et al.[7] for the translational diffusion coefficient of proteins in PEG solutions. However, for high molecular weight PEG $\left(r_p/R_g < 1\right)$ the data lies well off of this curve.

Instead of the radius of gyration the polymer, Kalwarczyk et al.[8] proposed a new variable defined $R_{eff}^{-2} = r_p^{-2} + R_g^{-2}$ as the scaling formula. In Figure SI-5 we show the experimentally measured relative diffusivities as D_0/D a function $2R_{eff}/\xi$. According to the results, we see a decently collapse of the data in samples where $r_p > R_g$. However, there is significant spread for high molecular weight polymers with $r_p < R_g$.

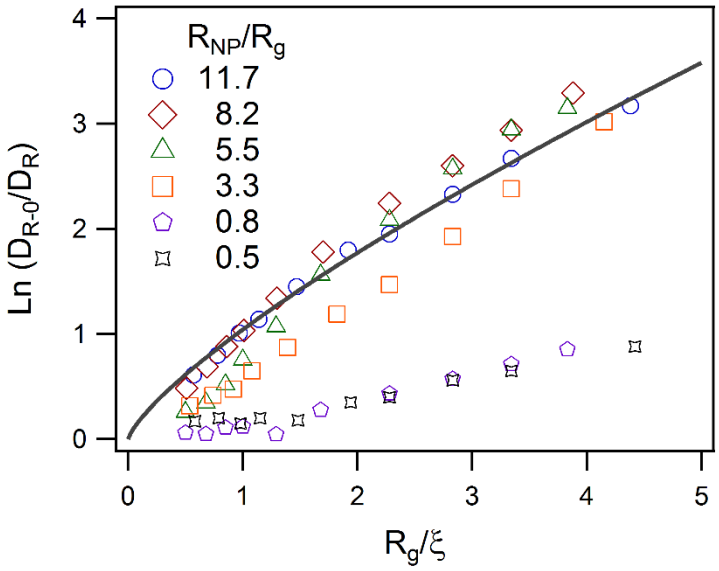

Figure SI-7. Relative diffusivities $\ln\left(D_{R-0}/D_R\right)$ as a function of R_g/ξ, which collapsed the data for large probes in Holyst et al.[7] The solid black line represents an exponential fit to the data with fitting parameters a = 0.77, b = 1.04. These ratio fails to collapse the data onto a single curve.

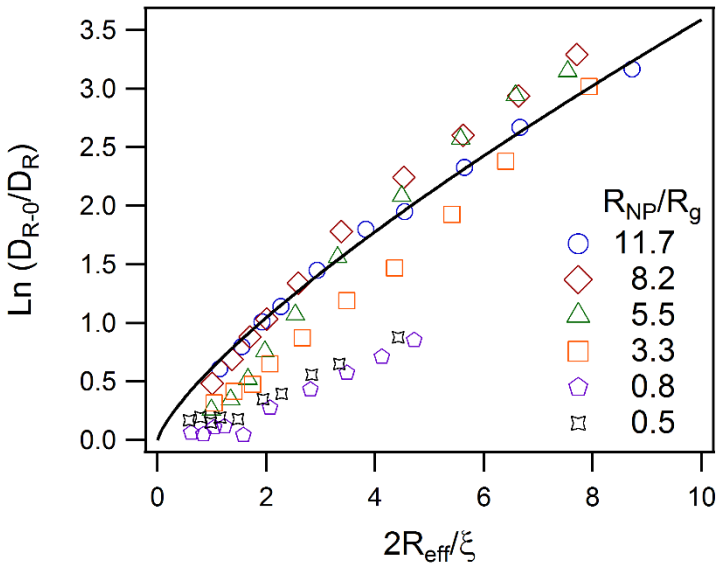

Figure SI-8. Relative diffusivities $\ln\left(D_{R-0}/D_R\right)$ as a function of $2R_{eff}/\xi$. The effective radius is defined as $R_{eff}^{-2} = r_p^{-2} + R_g^{-2}$, as proposed by Kalwarczyk et al.[8] The solid line represents an exponential fit with fitting parameters a = 0.77, b = 1.48. These ratio also fails to collapse the data onto a single curve

The existence of a depletion layer of solution polymer at the nanoparticle surface. To explore the existence of a depletion layer as a possible reason for the observed deviations of the rotational diffusion coefficient from the predictions of the SE relation, we estimated the thickness of the depletion layer in our system using the approximation by Fleer et al.[3, 9] for spheres. The thickness of the depletion layer depends on the polymer concentration according to the equation

$$\delta = 3\left(\frac{r_p^2\xi^2}{r_p^2+\xi^2}\right)^{0.5} \qquad (1)$$

where r_p is the radius of the nanoparticles and ξ the correlation length of the polymer in solution. The results of these calculations are summarized in Table SI-5. According to these calculations, as the polymer radius of gyration increases, the thickness of the depletion layer also increases to values larger than the diameter of the nanoparticles of the polymer, and is compressed as the concentration of the polymer increases. In solutions prepared with high molecular weight PEG and high c/c* the depletion layer decreases to the point where it is comparable to the depletion layer in low molecular weight PEG, however, the SE relation still fails to predict the rotational diffusion coefficient of the nanoparticles in this solutions. Furthermore, if the depletion layer where the explanation for our observations one would expect that as the concentration of PEG increases, the hydrodynamic drag on the nanoparticles would significantly increase due to the compression of the depletion zone. Imagine a solid sphere inside a liquid bubble dispersed in another medium of viscosity similar to the macroscopic viscosity. As the thickness of the gap between the solid and the outer medium increases the effective viscosity that determined the drag would increase. We did not see this effect because the rotational diffusivity remains relatively constant with increasing c/c*. Thus, the existence of a zone with lower polymer concentration surrounding the nanoparticle cannot be the only explanation for the observed deviation.

Table SI-5. Theoretical thickness of the depletion later proposed by Fleer et al.[3, 9]

c/c^* [approx.]	PEG 2 δ [nm]	PEG 4 δ [nm]	PEG 7 δ [nm]	PEG 17 δ [nm]	PEG 197 δ [nm]	PEG 363 δ [nm]
0.4	8.85	14.00	20.38	29.35	55.85	57.20
0.6	6.56	10.46	15.45	22.94	52.96	55.13
0.8	5.30	8.47	12.60	18.98	50.07	52.95
1.0	4.49	7.19	10.72	16.29	47.29	50.77
1.4	3.49	5.60	8.39	12.85	42.32	46.61
2.0	2.67	4.29	6.44	9.92	36.35	41.19
3.0	2.25	3.21	4.77	7.96	29.39	37.57
4.0	1.82	2.59	3.85	6.44	24.75	32.61
5.0	1.54	2.19	3.25	5.45	21.46	28.82
6.0	1.17	1.89	2.84	4.40	19.01	22.96

Hydrodynamic slip at the nanoparticle/solution interface. An alternative method to analyze the deviations is by introducing an equivalent slip effect at the solid-liquid interface.[10, 11] For particles in polymer matrices, Ganesan et al.[11] developed a model for the rotational diffusion coefficient of nanoparticles with hydrodynamic slip. Even though, Ganesan et al. [11] suggested that the formalism can be extended to polymer in solutions taking into consideration the polymer depletion effects, lacks of an explicit model. Thus, we consider the possibility that the functional form obtained by Ganesan et al.[11] of nanoparticles in the melt is valid for system. The slip phenomenon has been analyzed by Ganesan et al.[11] to explain deviations from the Stokes-Einstein relation of nanoparticles in polymer melts and polymer solutions. Phenomena such as autophobic dewetting of polymer in solution from the grafted polymer could result in hydrodynamic slip at the surface of the nanoparticles.[11-14] To estimate the slip length we used the model developed by Ganesan et al.[11] where the rotational diffusion coefficient of nanoparticles in a polymer melt where slip occurs is given by

$$D_R = \frac{(1+3\lambda)k_B T}{8\pi\eta_b r_p^3} \tag{2}$$

where η_b is the macroviscosity of the solution, r_p the hydrodynamic radius of the nanoparticles, and λ is the ratio of slip length to particle radius known as the dimensionless slip length.

We used Eq (2) to estimate the dimensionless hydrodynamic slip assuming the rotational diffusion coefficient of the nanoparticles measured by DMS. Table SI-6 summarizes these results. These calculations indicate that hydrodynamic slip would have an effect of the rotation diffusivity of the nanoparticles in polymer

solutions. The length of the slip is a function of polymer concentration and the molecular, and it has a greater effect on the rotational diffusion of nanoparticles in polymer solutions prepares with PEG 197 and PEG 363. Although various studies have shown that the no-slip boundary condition does not always apply for polymer melts,[11] its effect on colloidal particles in solutions has rarely been explored.[15, 16]

Table SI-6. Dimensionless slip length λ calculated from the experimental rotational diffusivity using Eq. (2).

c/c^* [approx.]	PEG 2 λ	PEG 4 λ	PEG 7 λ	PEG 17 λ	PEG 197 λ	PEG 363 λ
0.4	0.04	-0.018	0.068	0.031	0.165	0.154
0.6	0.05	-0.014	0.104	0.073	0.279	0.273
0.8	0.03	-0.015	0.101	0.119	0.420	0.461
1.0	0.11	0.007	0.058	0.120	0.549	0.596
1.4	0.14	-0.006	0.048	0.157	0.990	1.061
2.0	0.09	-0.009	0.012	0.194	1.225	1.721
3.0	0.18	-0.013	0.004	0.272	2.217	2.987
4.0	0.12	-0.014	-0.034	0.248	3.586	4.826
5.0	0.18	-0.021	-0.046	0.183	5.286	7.443
6.0	-0.33	-0.042	-0.021	0.125	7.287	9.645

Rotational Hydrodynamic Drag and Diffusivity of a Particle Surrounded by a Depletion Layer

Consider the situation in Figure 6a shows a schematic representation of the system. In this figure, the magnetic nanoparticles, represented by the solid black sphere, are surrounded by a depletion zone where the polymer concentration is lower. Outside the depletion zone, there is a uniform polymer solution. For simplicity, the viscosities of the inner and outer regions are assumed to be uniform. By symmetry about the z –axis, no quantity depends on φ. Therefore, the velocity v_φ is independent of φ, and the velocity field is such that $\mathrm{v}_\mathrm{r} = \mathrm{v}_\theta = 0$ from the continuity equation in spherical coordinates. Consequently, the r and θ components of Stokes' equation are reduced to $\partial \mathscr{P} \partial r = \partial \mathscr{P} \partial \theta = 0$, which indicate that the dynamic pressure is constant throughout the fluid. The φ component of the Stokes' equation becomes

$$0 = \frac{1}{r^2}\frac{\partial}{\partial r}\left(r^2 \frac{\partial v_\varphi}{\partial r}\right) + \frac{1}{r^2 \sin\theta}\frac{\partial}{\partial \theta}\left(\sin\theta \frac{\partial v_\varphi}{\partial \theta}\right) - \frac{v_\varphi}{r^2 \sin^2\theta} \tag{3}$$

taking into consideration that v_φ depends on θ and r, v_φ can be expressed as

$$v_\varphi(r,\theta) = f(r)\sin\theta \text{ at } R < r < R + \delta \tag{4}$$

$$v_\varphi(r,\theta) = g(r)\sin\theta \text{ at } r > R + \delta \tag{5}$$

where δ is the thickness of the depletion layer around the sphere.

Substituting the assumed forms of v_φ Eq. (3) one obtains

$$\frac{d}{dr}\left(r^2 \frac{df}{\partial r}\right) - 2f = 0 \tag{6}$$

$$\frac{d}{dr}\left(r^2 \frac{dg}{\partial r}\right) - 2g = 0 \tag{7}$$

The general solutions of these differential equations are

$$f(r) = ar + br^{-2} \tag{8}$$

$$g(r) = cr + dr^{-2} \tag{9}$$

where a, b, c, and d are constants. The boundary conditions for the velocity are

$v_r = 0;$ $v_\theta = 0;$ $v_\varphi = \omega R \sin\theta$ at $r = R$

$v_r = 0;$ $v_\theta = 0;$ $v_\varphi^-(R+\delta) = v_\varphi^+(R+\delta)$ at $r = R + \delta$

Then, taking into consideration these boundary conditions one obtains, at $r = R$,

$$f(R) = aR + bR^{-2} = \omega R \tag{10}$$

at the interface $r = R + \delta$

$$a(R+\delta) + b(R+\delta)^{-2} = c(R+\delta) + d(R+\delta)^{-2} \tag{11}$$

and, at $r = \infty$

$$g(\infty) = 0 \tag{12}$$

hence $c = 0$.

With $v_\varphi(\theta, r)$ being the only non-zero velocity component, the shear stress is

$$\tau_{r\varphi} = \tau_{\varphi r} = \mu\left[r\frac{\partial}{\partial r}\left(\frac{v_\varphi}{r}\right)\right] \tag{13}$$

and at $r = R + \delta$

$$\mu_1\left[r\frac{\partial}{\partial r}\left(\frac{f}{r}\right)\right]_{R+\delta} = \mu_2\left[r\frac{\partial}{\partial r}\left(\frac{g}{r}\right)\right]_{R+\delta} \tag{14}$$

where μ_1 is the viscosity of the solution in the depletion layer and μ_2 is the viscosity of the polymer solution. Here we will assume that the viscosity in the polymer depletion zone corresponds to the solvent viscosity.[9] From Eq. (14) one obtains

$$\frac{\mu_1}{\mu_2} = \frac{d}{b} \tag{15}$$

The integration constants *a, b, c,* and *d* can be shown to be given by

$$a = \omega - \frac{\omega}{1 + \left(\frac{\mu_1}{\mu_2} - 1\right)\left(\frac{R}{R+\delta}\right)^3} \tag{16}$$

$$b = \frac{\omega R^3}{1 + \left(\frac{\mu_1}{\mu_2} - 1\right)\left(\frac{R}{R+\delta}\right)^3} \tag{17}$$

$$c = 0 \tag{18}$$

$$d = \frac{\mu_1}{\mu_2}\frac{\omega R^3}{1 + \left(\frac{\mu_1}{\mu_2} - 1\right)\left(\frac{R}{R+\delta}\right)^3} \tag{19}$$

Therefore, the expression for the velocity in the depletion layer $R < r < R + \delta$ is

$$v_\varphi(r,\theta) = \omega r - \frac{\omega r}{1 + \left(\frac{\mu_1}{\mu_2} - 1\right)\left(\frac{R}{R+\delta}\right)^3} + \frac{\omega \sin\theta}{r^2\left[1 + \left(\frac{\mu_1}{\mu_2} - 1\right)\left(\frac{R}{R+\delta}\right)^3\right]} \tag{20}$$

whereas the velocity in the outer region $r > R + \delta$ is

$$v_\varphi(r,\theta) = \frac{\mu_1}{\mu_2}\frac{\omega R^3}{1 + \left(\frac{\mu_1}{\mu_2} - 1\right)\left(\frac{R}{R+\delta}\right)^3}\cdot\frac{\sin\theta}{r^2} \tag{21}$$

To calculate the torque at the particle surface, we evaluate the shear stress at $r = R$

$$\tau_{r\varphi} = \mu\left[r\frac{\partial}{\partial r}\left(\frac{v_\varphi}{r}\right)\right]\Bigg|_{r=R} = -\frac{3\mu_1\omega\sin\theta}{1+\left(\frac{\mu_1}{\mu_2}-1\right)\left(\frac{R}{R+\delta}\right)^3} \tag{22}$$

Then, the torque is

$$G = 2\pi R^3\int_0^\pi \tau_{r\varphi}\Big|_{r=R}\sin^2\theta\, d\theta = -\frac{8\pi\mu_1\omega R^3}{1+\left(\frac{\mu_1}{\mu_2}-1\right)\left(\frac{R}{R+\delta}\right)^3} = \xi_R\omega \tag{23}$$

where the rotational friction coefficient ξ_R is

$$\xi_R = \frac{8\pi\mu_1 R^3}{1+\left(\frac{\mu_1}{\mu_2}-1\right)\left(\frac{R}{R+\delta}\right)^3} \tag{24}$$

Assuming that the Einstein formalism for the rotational diffusivity applies albeit with the rotational hydrodynamic drag from Eq. (24), that is $D_R = k_BT/\xi_R$, we obtain an expression for the rotational diffusion coefficient experienced by a solid sphere in a polymer solution including the effect of the depletion zone

$$D_R = \frac{k_BT}{8\pi\mu_1 R^3}\left[1+\left(\frac{\mu_1}{\mu_2}-1\right)\left(\frac{R}{R+\delta}\right)^3\right] \tag{25}$$

References

1. Rubinstein, M.; Colby, R. H., *Polymer Physics*. OUP Oxford: 2003.
2. Fetters, L. J.; Lohse, D. J.; Colby, R. H., Chain Dimensions and Entanglement Spacings. In *Physical Properties of Polymers Handbook*, Mark, J. E., Ed. Springer New York: New York, NY, 2007; pp 447-454.
3. Ziebacz, N.; Wieczorek, S. A.; Kalwarczyk, T.; Fialkowski, M.; Holyst, R., Crossover regime for the diffusion of nanoparticles in polyethylene glycol solutions: influence of the depletion layer. *Soft Matter* **2011,** *7* (16), 7181-7186.
4. Odijk, T., Depletion theory of protein transport in semi-dilute polymer solutions. *Biophys J* **2000,** *79* (5), 2314-2321.
5. Kalwarczyk, T.; Sozanski, K.; Ochab-Marcinek, A.; Szymanski, J.; Tabaka, M.; Hou, S.; Holyst, R., Motion of nanoprobes in complex liquids within the framework of the length-scale dependent viscosity model. *Adv Colloid Interfac* **2015,** *223*, 55-63.
6. Wisniewska, A.; Sozanski, K.; Kalwarczyk, T.; Kedra-Krolik, K.; Pieper, C.; Wieczorek, S. A.; Jakiela, S.; Enderlein, J.; Holyst, R., Scaling of activation energy for macroscopic flow in poly(ethylene glycol) solutions: Entangled - Non-entangled crossover. *Polymer* **2014,** *55* (18), 4651-4657.
7. Holyst, R.; Bielejewska, A.; Szymanski, J.; Wilk, A.; Patkowski, A.; Gapinski, J.; Zywocinski, A.; Kalwarczyk, T.; Kalwarczyk, E.; Tabaka, M.; Ziebacz, N.; Wieczorek, S. A., Scaling form of viscosity at all length-scales in poly(ethylene glycol) solutions studied by fluorescence correlation spectroscopy and capillary electrophoresis. *Physical Chemistry Chemical Physics* **2009,** *11* (40), 9025-9032.
8. Kalwarczyk, T.; Zięba cz, N.; Bielejewska, A.; Zaboklicka, E.; Koynov, K.; Szymański, J.; Wilk, A.; Patkowski, A.; Gapiński, J.; Butt, H.-J.; Hołyst, R., Comparative Analysis of Viscosity of Complex Liquids and Cytoplasm of Mammalian Cells at the Nanoscale. *Nano Lett* **2011,** *11* (5), 2157-2163.
9. Fleer, G. J.; Skvortsov, A. M.; Tuinier, R., Mean-field equation for the depletion thickness. *Macromolecules* **2003,** *36* (20), 7857-7872.
10. Fan, T. H.; Dhont, J. K. G.; Tuinier, R., Motion of a sphere through a polymer solution. *Phys Rev E* **2007,** *75* (1).
11. Ganesan, V.; Pryamitsyn, V.; Surve, M.; Narayanan, B., Noncontinuum effects in nanoparticle dynamics in polymers. *J Chem Phys* **2006,** *124* (22).
12. Borukhov, I.; Leibler, L., Enthalpic stabilization of brush-coated particles in a polymer melt. *Macromolecules* **2002,** *35* (13), 5171-5182.
13. Maas, J. H.; Fleer, G. J.; Leermakers, F. A. M.; Stuart, M. A. C., Wetting of a polymer brush by a chemically identical polymer melt: Phase diagram and film stability. *Langmuir* **2002,** *18* (23), 8871-8880.
14. Matsen, M. W., Scaling behavior of a brush-homopolymer interface in the limit of high grafting density. *J Chem Phys* **2005,** *122* (14).
15. Granick, S.; Zhu, Y.; Lee, H., Slippery questions about complex fluids flowing past solids. *Nat Mater* **2003,** *2* (4), 221-227.
16. Begam, N.; Chandran, S.; Sprung, M.; Basu, J. K., Anomalous Viscosity Reduction and Hydrodynamic Interactions of Polymeric Nanocolloids in Polymers. *Macromolecules* **2015,** *48* (18), 6646-6651.